Journal of Systems Engineering and Electronics
Vol. PP, No. 99, June 2024, pp.1 – 12

Generalized multiple-mode prolate spheroidal wave functions multi-carrier waveform with index modulation

XU Zhichao[1,2], LU Faping[2,*], ZHANG Lifan[3], YANG Dongkai[1], LIU Chuanhui[2], KANG Jiafang[2], AN Qi[2], and ZHANG Zhilin[2]

1. School of Electronical and Information Engineering, Beijing University of Aeronautics and Astronautics, Beijing 100191, China; 2. Naval Aviation University, Yantai 264001, China; 3. Unit 92664 of the PLA, Qingdao 266100, China

Abstract: A generalized multiple-mode prolate spherical wave functions (PSWFs) multi-carrier with index modulation approach is proposed with the purpose of improving the spectral efficiency of PSWFs multi-carrier systems. The proposed method, based on the optimized multi-index modulation, does not limit the number of signals in the first and second constellations and abandons the concept of limiting the number of signals in different constellations. It successfully increases the spectrum efficiency of the system while expanding the number of modulation symbol combinations and the index dimension of PSWFs signals. The proposed method outperforms the PSWFs multi-carrier index modulation method based on optimized multiple indexes in terms of spectrum efficiency, but at the expense of system computational complexity and bit error performance. For example, with n=10 subcarriers and a bit error rate of 1×10^{-5}, spectral efficiency can be raised by roughly 12.4%.

Keywords: prolate spherical wave function (PSWF), generalized multiple-mode, index modulation, spectral efficiency.

DOI: 10.23919/JSEE.2024.000044

1. Introduction

The exponential growth of information transmission is a direct consequence of society's progression towards digitization. Based on the Edholm law, it is projected that the volume of information transmission will attain the terabyte (TB) level by the year 2030 [1,2]. The pursuit of achieving high spectral efficiency (SE) and energy aggregation for information transmission has emerged as a prominent research area in the field of beyond 5G (B5G)/6G communication [3−5]. Various forms of high SE index modulation, such as spatial index modulation, spatial time index modulation, and frequency domain index modulation, have been successively introduced in the context of information mapping. The enhancement of spectral efficiency is achieved by increasing the number of modulation symbol combinations through the utilization of various techniques such as mapping bit information via index antennas, spatial time resources, subcarriers, and other relevant means. One technique that can significantly increase the number of modulation symbol permutations by indexing subcarriers is subcarrier index modulation (SIM). SIM is a frequency domain index modulation representation that can be easily employed with technologies like orthogonal frequency division multiplexing (OFDM). Basar et al. [6] initially incorporated it into OFDM due to its favorable compatibility with existing communication systems, efficient utilization of system bandwidth, and robustness against multipath interference. As a promising technology for facilitating B5G/6G networks, it has garnered significant attention from experts and scholars in relevant domains [7−9].

Various high-energy aggregation signal waveforms, such as universal filtered multi carrier (UFMC) [10], generalized frequency division multiplexing (GFDM) [11], filter bank multi-carrier (FBMC) [12], and multi-carrier modulation based on PSWFs (PSWFs-MCM)[13], are proposed at the signal waveform level. These waveforms are utilized either through filtering techniques or by employing them as carriers to mitigate out-of-band energy leakage. Among the various options, MCM-PSWFs [13,14] employ PSWFs signals due to their exceptional fundamental properties, including perfect orthogonally, time-domain parity symmetry, and optimal time-frequency energy aggregation [15,16], as the foundational waveform. In contrast to emerging B5G/6G alternatives like UFMC [10], GFDM [11], and FBMC, MCM-PSWFs possess several advantages including flexi-

Manuscript received January 24, 2024.
*Corresponding author.
This work was supported by the China National Postdoctoral Program for Innovative Talents (BX20200039) and the Special Fund Project of "Mount Taishan Scholars" Construction Project in Shandong Province (ts20081130).

ble signal waveform design, high energy aggregation, and high SE [15]. These advantages align well with the demands of information transmission, particularly in terms of high SE and energy aggregation. The technology exhibits significant promise and future possibilities for practical implementation [13,14]. Tong et al. and Murugesan et al. recognized its potential as a waveform scheme for B5G/6G [17,18].

The integration of PSWFs-MCM with SIM is anticipated to yield simultaneous enhancements in both SE and energy aggregation. This was also confirmed in [19], where they included SIM into MCM-PSWFs and presented an MCM technique based on PSWFs with signal grouping optimization (MCM-PSWFs-SGO). This method initially focuses on optimizing the grouping of PSWFs signals. Subsequently, it employs signal index and pulse amplitude modulation (PAM) to facilitate information mapping in two dimensions. It not only effectively utilizes the characteristics of index modulation technology, which can greatly enhance the SE of information transmission, but also integrates the benefits of flexible and high energy aggregation in the design of PSWFs signal waveform, with high energy aggregation and high SE. However, because the idle subcarriers of MCM-PSWFs-SGO do not contain any modulation symbols, the improvement of its system SE is limited to some amount. Following that, Wang et al. [20] presented MCM-PSWFs with dual mode (DM-MCM-PSWFs). On the basis of MCM-PSWFs-SGO, this approach adds a second constellation and utilizes silence subcarriers in MCM-PSWFs-SGO to transmit modulation symbols mapped from the second constellation. It can successfully enhance system bandwidth utilization and bit error rate (BER) performance when the signal to noise ratio (SNR) is high without modifying the peak to average power ratio (PAPR) or energy aggregation, but at the expense of system complexity. Then, in [21], MCM-PSWFs with improved index multiple mode were proposed, called index multicarrier modulation based on PSWFs with better index multiple-mode (BIM-MCM-PSWFs). This approach adds a third constellation based on DM-MCM-PSWFs and enhances system SE by organizing and merging the subcarriers in each sub-block after grouping. However, the number of active subcarriers is set in the three approaches discussed above, limiting future increase of system bandwidth utilization. Reference [22] suggested an MCM approach for PSWFs based on generalized signal indexes, called MCM-PSWFs with generalized index modulation (MCM-PSWFs GIM), which does not limit the number of active signals and has higher system SE when compared to a fixed number of active signals.

This paper proposes a method that combines BIM-MCM-PSWFs with generalized signal index, dubbed generalized multiple-mode PSWFs multi-carrier with index modulation (GMM-PSWFs-IM). This approach merely fixes the number of active signal paths in the third constellation of the original BIM-MCM-PSWFs, and the number of signal paths in the first and second constellations is no longer fixed. It can increase the number of modulation symbol possibilities and, in the case of a large number of subcarriers, improve the system SE at the expense of compromising BER performance and computational complexity accordingly. The following are this paper's main contributions:

To begin, the GMM-PSWFs-IM approach is proposed, which employs a "dual signal index+three constellation maps" information mapping structure, allowing to increase the number of modulation symbol combinations while also obtaining greater system SE. This method uses the "signal index (fixed activation signal number)+generalized signal index (unfixed activation signal number)" for the second signal index to balance the system BER performance. Simultaneously, constellation maps that do not overlap and are easily identifiable in order to separate signals activated by two signal indices is built. In comparison with the approaches such as BIM-MCM-PSWFs, DM-MCM-PSWFs, and MCM-PSWFs-SGO, the proposed method achieves a better balance between system SE and BER performance.

Second, we offer a method for detecting and demodulating GMM-PSWFs-IM modulation signals using maximum likelihood (ML). The suggested technique first detects modulation symbols carried by distinct branch PSWFs signals using fast Fourier transform (FFT)-based PSWFs signal frequency domain detection [13]. Furthermore, to obtain excellent signal index detection performance, the ML algorithm is applied. The bit information transmitted by the transmitter is then reconstituted by modulating symbol inverse mapping.

Third, the suggested approach's system SE is provided and the benefits of the proposed technique in terms of system SE and BER performance are demonstrated by combining it with the minimum Euclidean distance (MED). The theoretical analysis's correctness is confirmed through numerical simulation. It is worth noting that the above benefits are obtained at the expense of the system complexity that current hardware can withstand, and with the continuous improvement of computing power, particularly the improvement of B5G/6G terminal computing power, the proposed method will be easily realized.

2. Principle of GMM-PSWFs-IM

The key factor limiting future system SE improvement in the BIM-MCM-PSWFs is that the number of active sig-

nals in the signal index scheme is fixed, severely limiting the number of modulation symbol combinations. Simultaneously, if the number of activation signals is not fixed, i.e., the generalized signal index, the system BER performance is lower and the signal index detection complexity is greater. As a result, GMM-PSWFs-IM uses a dual signal index, with only a portion of the PSWFs signal undergoing GIM, which enhances system SE while also taking BER performance and detection complexity into account.

Fig. 1 depicts the schematic diagram of GMM-PSWFs-IM modulation signal generation at the transmitter, which includes two signal indices, the primary signal index (fixed number of activation signal) and the generalized signal index (unfixed number of activation signal), as well as three constellation diagrams, constellations A, B, and C. The proposed technique is separated into inphase/quadrature(I/Q) branches and employs the same signal index structure. The primary signal index is in charge of the first signal index, which activates a set number of signals and controls constellation C to translate bit information to modulation symbols. The generalized signal index is in charge of the second signal index, which is responsible for indexing the inactive signals in the first signal index without limiting the amount of active signals. It also directs constellation A to map bit information to the modulation symbols corresponding to active signals, and constellation B to map bit information to inactive signal modulation symbols.

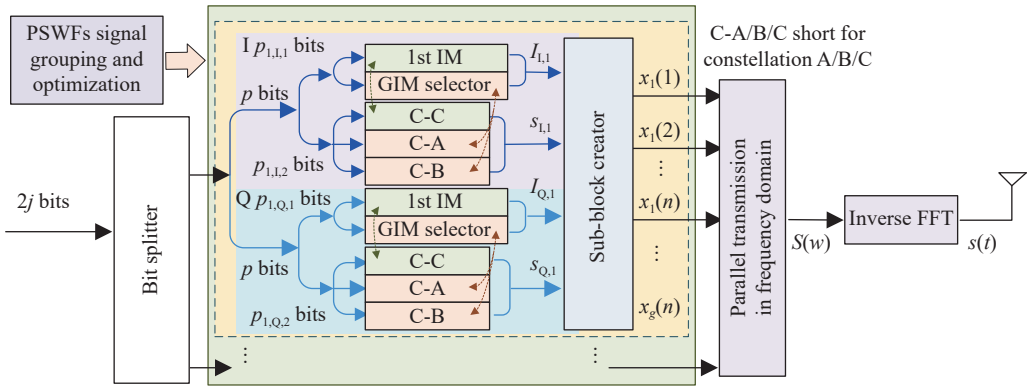

Fig. 1 Principle block diagram of GMM-PSWFs-IM

In addition, because parameters such as the number of signal packets, the number of signals in each group, the number of modulation bases, and the number of activation signals directly determine the overall performance of the system, the overall system must be designed and selected based on the size of available time-frequency resources and the system's overall performance requirements [19]. For the sake of simplicity, the PSWFs signal is assumed to be a low-pass PSWFs signal with signal duration of T, bandwidth of $B/2$, number of signal groups of g, number of signals in each group of n, number of signals selected for the first index of k, number of signal paths selected for the second index of $m, m \in [0, n-k]$, and all three constellations with M-ary modulation.

At the transmitter, the PSWFs signals are optimized and grouped based on $c-l$ (the number of signals, and $l \in [1, c-1], c = BT$), g (the number of signal packets), n (the number of signals per group), and k (the number of activation signal) that can be used for information transmission [19]. At the same time, divide the input $2j$ information bits to be transmitted into g groups on average, each group containing $p' = 2j/g = p_{\mathrm{I}} + p_{\mathrm{Q}}$. Among them, $p_{\mathrm{I}} = p_{\mathrm{Q}} = p$, $p_{\mathrm{I}} = p_{\alpha,\mathrm{I},1} + p_{\alpha,\mathrm{I},2}$, $p_{\mathrm{Q}} = p_{\alpha,\mathrm{Q},1} + p_{\alpha,\mathrm{Q},2}$, $\alpha \in [1, g]$, and $p_{\alpha,\mathrm{I/Q},1}$ represents the information carried by the index part of the I/Q branch signal, and $p_{\alpha,\mathrm{I/Q},2}$ represents the information carried by the modulation symbols corresponding to the three constellations. Then, perform constellation design and bit information mapping to generate modulation symbols and generate modulation signals.

2.1 PSWFs selection and grouping

PSWFs are a class of non-sinusoidal function sets [23], which have excellent characteristics such as completeness, orthogonality, optimal band-limited signal, time and bandwidth, and flexible and controllable spectrum. PSWFs can be expressed as

$$\int_{-T/2}^{T/2} \varphi_n(\tau) h(t) \mathrm{d}\tau = \lambda_n \varphi_n(t). \tag{1}$$

It is worth noting that $c = TB$ is the time-bandwidth product, $\psi_n(c,t)$ is the nth order PSWFs, and λ_n is the eigenvalue of the nth order PSWFs. $h(t)$ represents the time domain response of the ideal filter, $\varphi_n(t)$ represents baseband PSWFs at $h(t) = \sin(Bt)/\pi t$, and $\varphi_n(t)$ repre-

sents pass band PSWFs at $h(t)=2f_h\text{sinc}(2f_ht)-2f_l\text{sinc}(2f_lt)$, while f_h and f_l respectively denote the upper and lower limit frequency of PSWFs.

PSWFs selection and grouping have been introduced in detail in [19] and [22], thus we do not explain it in this paper. The proposed method begins with the goal of ensuring signal energy aggregation, that is, the first ng order PSWFs signals are selected for information transmission, namely $\Phi\{\varphi_i(t)\}$ $(i=0,1,\cdots,ng-1)$, based on the number of signal groups g and the number of signal paths n in each group. Among them, $\varphi_i(t)$ is the ith order PSWFs signal. Furthermore, the ng branch signals are grouped according to the signal order, with order signal from $(\alpha-1)n$ to αn serving as the $\alpha=1,2,\cdots,g$ group, and the n branch signals within each group are numbered form 1 to n.

2.2 Signal index and constellation scheme design

As shown in Fig. 2, GMM-PSWFs-IM employs a "signal index (fixed number of activation signal) and the generalized signal index (unfixed number of activation signal)" scheme. The fixed activation signal index (classical called IM), i.e., the first signal index, chooses k activations from n subcarriers and controls constellation C to generate modulation symbols corresponding to the activation signal. The generalized signal index (also known as the second signal index, classical called GIM [24]) selects activation signals at random from $n-k$ subcarriers and controls constellation A to generate modulation symbols corresponding to active signals, while constellation B generates modulation symbols corresponding to inactive signals. Furthermore, because the proposed method uses two signal indexes, correctly distinguishing the second signal index becomes critical to recovering the signal index and modulation symbol carrying bit information at the receiving end. The dual signal index necessitates the use of non-overlapping and distinct constellation maps, particularly constellation maps C, A, and B, to address the aforementioned issues. As shown in Fig. 2, the constellation points of constellation C are located at the outermost point, while the constellation points of constellations A and B are located inside.

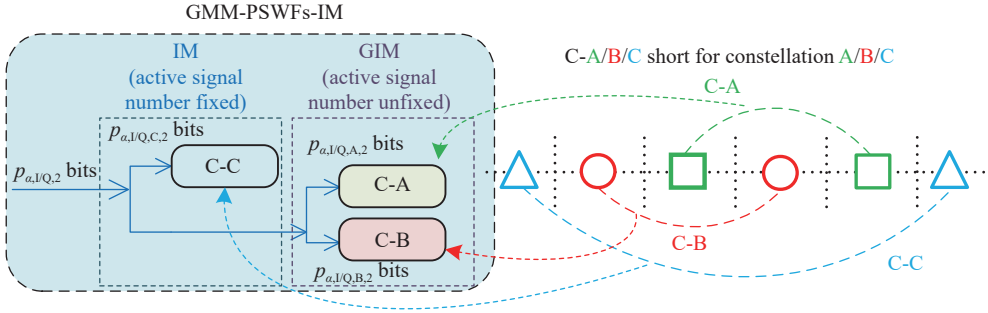

Fig. 2 Mapping principle of GMM-PSWFs-IM

It is worth noting that, when compared to the signal index with a fixed number of activation signals, the generalized signal index with an unfixed number of signals has a relatively low system BER performance. In the meantime, a signal index with a fixed number of activation signals can also be considered a type of generalized signal index. As a result, the proposed GMM-PSWFs-IM's generalized signal index can also fix the number of active signal paths.

For signal index with fixed activation signal paths, the permutation and combination method is used to design the PSWFs signal index scheme. When the number of active PSWFs signal paths is k, all signal index schemes $Z\in[0,C_n^k-1]$ can be represented by a sequence $J=\{d_k,d_{k-1},\cdots,d_1\}$ of length $k\in[1,n]$[6]. Among them, $d_k>d_{k-1}>\cdots>d_1>0$ can be obtained by

$$Z=C(d_k,k)+C(d_{k-1},k-1)+\cdots+C(d_1,1) \tag{2}$$

where Z is the decimal number corresponding to the sequence of bit information.

For the generalized signal index with an unfixed number of the signal, the signal index scheme is the set of signal index schemes corresponding to the fixed number of activation signal with different activation signal paths [25], i.e.,

$$Z=\{Z_1,Z_2,\cdots,Z_m\} \tag{3}$$

where $Z_i=C(d_{k_i},k_i)+C(d_{k_i-1},k_i-1)+\cdots+C(d_{k_1},1),d_{k_i}>\cdots>d_{k_1}>0,i=1,2,\cdots,m$, the same processing as in (2) is used. Table 1 provides the signal index scheme for GMM-PSWFs-IM with n=3.

Table 1 Mapping scheme of GMM-PSWFs-IM

Bit information	Signal index	Subcarrier mapping
[0,0,0]	{3,1,2}	$\{s_{\mathrm{I}}^{\mathrm{C}}(1), s_{\mathrm{I}}^{\mathrm{A}}(1), s_{\mathrm{I}}^{\mathrm{B}}(1)\}$
[0,0,1]	{3,2,1}	$\{s_{\mathrm{I}}^{\mathrm{C}}(1), s_{\mathrm{I}}^{\mathrm{B}}(1), s_{\mathrm{I}}^{\mathrm{A}}(1)\}$
[0,1,0]	{1,3,2}	$\{s_{\mathrm{I}}^{\mathrm{A}}(1), s_{\mathrm{I}}^{\mathrm{C}}(1), s_{\mathrm{I}}^{\mathrm{B}}(1)\}$
[0,1,1]	{2,3,1}	$\{s_{\mathrm{I}}^{\mathrm{B}}(1), s_{\mathrm{I}}^{\mathrm{C}}(1), s_{\mathrm{I}}^{\mathrm{A}}(1)\}$
[1,0,0]	{1,2,3}	$\{s_{\mathrm{I}}^{\mathrm{A}}(1), s_{\mathrm{I}}^{\mathrm{B}}(1), s_{\mathrm{I}}^{\mathrm{C}}(1)\}$
[1,0,1]	{2,1,3}	$\{s_{\mathrm{I}}^{\mathrm{B}}(1), s_{\mathrm{I}}^{\mathrm{A}}(1), s_{\mathrm{I}}^{\mathrm{C}}(1)\}$
[1,1,0]	{1,1,3}	$\{s_{\mathrm{I}}^{\mathrm{A}}(1), s_{\mathrm{I}}^{\mathrm{A}}(2), s_{\mathrm{I}}^{\mathrm{C}}(1)\}$
[1,1,1]	{2,2,3}	$\{s_{\mathrm{I}}^{\mathrm{B}}(1), s_{\mathrm{I}}^{\mathrm{B}}(2), s_{\mathrm{I}}^{\mathrm{C}}(1)\}$

2.3 Bit information grouping and signal index

Based on the number of PSWFs signal groups, denoted as "g", the number of signal paths per group, denoted as "n", and the number of activated PSWFs signal paths by the first signal index, denoted as "k", the 2nd signal index scheme is designed using (1) and (2) (see [19] and [22] for details, which will not be repeated here) to determine the amount of bit information carried by the signal index and modulation symbol. Among them, the total amount of information that group g PSWFs signals can carry is

$$j = 2gp_{\alpha,\mathrm{I/Q}} \tag{4}$$

where $p_{\alpha,\mathrm{I/Q}}$ is the amount of information that can be carried by the I/Q branch of each n-order PSWFs signal, i.e.,

$$p_{\alpha,\mathrm{I/Q}} = \left\lfloor \log_2\left(C_n^k M^k\right) \right\rfloor + \lfloor (n-k)\log_2(1+M) \rfloor \tag{5}$$

where $\lfloor\cdot\rfloor$ represents rounding down. In addition, the information carried by the I/Q branch signal index and constellation corresponding modulation symbols of each n-order PSWFs signal is

$$\begin{cases} p_{\alpha,\mathrm{I/Q},1} = 2gp_{\alpha,\mathrm{I/Q}} - n\log_2 M \\ p_{\alpha,\mathrm{I/Q},2} = p_{\alpha,\mathrm{I/Q,A},2} + p_{\alpha,\mathrm{I/Q,B},2} + p_{\alpha,\mathrm{I/Q,C},2} = n\log_2 M \end{cases} \tag{6}$$

where $p_{\alpha,\mathrm{I/Q},2}$ represents the amount of information carried by the modulation symbols corresponding to the three constellations, while $p_{\alpha,\mathrm{I/Q,A},2}, p_{\alpha,\mathrm{I/Q,B},2}, p_{\alpha,\mathrm{I/Q,C},2}$ represent the amount of information carried by the modulation symbols generated by the constellation A, B and C, respectively.

According to $p_{\alpha,\mathrm{I},1}, p_{\alpha,\mathrm{Q},1}$ and signal index schemes, activate k signals from n-order PSWFs signals in the αth ($\alpha \in [1,g]$) sub block to load modulation symbols generated by constellation C. Randomly activate signals from the remaining ($n-k$)-order PSWFs signals to load the modulation symbols generated by constellation A, while the inactive signals are used to load the modulation symbols generated by constellation B, as shown in Fig. 3. $S_{\alpha,\mathrm{I,A}}$, $S_{\alpha,\mathrm{I,B}}$, $S_{\alpha,\mathrm{I,C}}$ represent the set of modulation symbols-generated by three constellation maps in branch I. $S_{\alpha,\mathrm{Q,A}}$, $S_{\alpha,\mathrm{Q,B}}$, $S_{\alpha,\mathrm{Q,}C}$ represent the set of modulation symbolsgenerated by three constellation maps in branch Q. Correspondingly, the signal index of the αth sub block can be represented as

$$I_{\mathrm{I},\alpha} = \{ i_{\mathrm{I},\alpha,1,\mathrm{CM}}, i_{\mathrm{I},\alpha,2,\mathrm{CM}}, \cdots, i_{\mathrm{I},\alpha,n,\mathrm{CM}} \}, \tag{7}$$

$$I_{\mathrm{Q},\alpha} = \{ i_{\mathrm{Q},\alpha,1,\mathrm{CM}}, i_{\mathrm{Q},\alpha,2,\mathrm{CM}}, \cdots, i_{\mathrm{Q},\alpha,n,\mathrm{CM}} \}, \tag{8}$$

where $\mathrm{CM} = [\mathrm{A},\mathrm{B},\mathrm{C}]$, $I_{\mathrm{I/Q},\alpha,\gamma,M}$ represents the αth sub block, with the PSWFs signal index numbered $\gamma \in [1,n]$. When CM=A, it indicates that the modulation symbol generated by constellation A is loaded into the PSWFs signal with the number $\gamma \in [1,n]$. Similarly, when CM=B and C, they represent the modulation symbols generated by loading the modulation symbols as constellation B and constellation C, respectively.

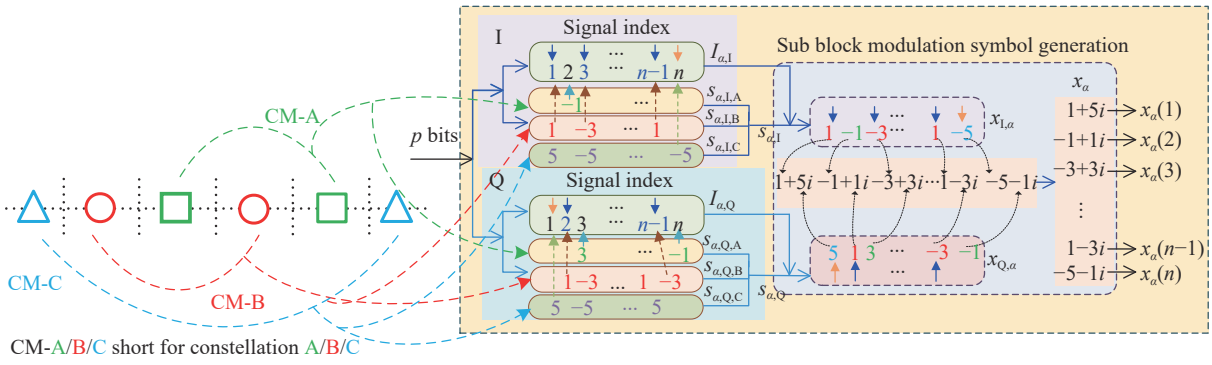

Fig. 3 GMM-PSWFs-IM modulation symbol loading process

2.4 Modulation symbols and modulation signal generation

Based on the I/Q branch bit information $P_{\alpha,\mathrm{I},2}$, $P_{\alpha,\mathrm{Q},2}$, constellations A, B, and C generate corresponding modulation symbols, i.e.,

$$\boldsymbol{S}_{\alpha,\mathrm{I}} = \{s_{\mathrm{I}}^{\mathrm{A}}(\lambda), s_{\mathrm{I}}^{\mathrm{B}}(\beta), s_{\mathrm{I}}^{\mathrm{C}}(\nu)\}, \tag{9}$$

$$\boldsymbol{S}_{\alpha,\mathrm{Q}} = \{s_{\mathrm{Q}}^{\mathrm{A}}(\lambda), s_{\mathrm{Q}}^{\mathrm{B}}(\beta), s_{\mathrm{Q}}^{\mathrm{C}}(\nu)\}, \tag{10}$$

where, λ=1, 2, ⋯, $n-k-m$, β=1,2,⋯,m, m=[1,2,⋯,$n-1$] and v=k, $s^{\mathrm{C}}_{\mathrm{I/Q}}(v)$ represents the modulation symbol corresponding to constellation C, while $s^{\mathrm{A}}_{\mathrm{I/Q}}(\lambda)$ and $s^{\mathrm{B}}_{\mathrm{I/Q}}(\beta)$ represent the modulation symbols corresponding to constellation A and B, respectively.

Furthermore, the modulation symbols $\boldsymbol{X}=[\boldsymbol{X}_1,\boldsymbol{X}_2,\cdots,\boldsymbol{X}_g]$ corresponding to all g sub blocks and ng branch PSWFs signals are generated, as shown in Fig. 3.

Among them, $\boldsymbol{X}_\alpha \in \mathbf{C}^{n\times 1}$ is the modulation symbol of the sub block, i.e.,

$$\boldsymbol{X}_\alpha=[x_{\mathrm{I},\alpha}(1)+ix_{\mathrm{Q},\alpha}(1),x_{\mathrm{I},\alpha}(2)+ix_{\mathrm{Q},\alpha}(2),\cdots,x_{\mathrm{I},\alpha}(n)+ix_{\mathrm{Q},\alpha}(n)] \tag{11}$$

where $x_{\mathrm{I/Q},\alpha}(\gamma)\in \boldsymbol{S}_{\alpha,\mathrm{I/Q}}$ and $\gamma\in[1,n]$.

In order to be better compatible with communication systems such as long term evolution (LTE) and Wi-Fi that use FFT and inverse FFT (IFFT) signal processing modules, and to further reduce signal processing complexity, the proposed method adopts a frequency domain generation method of PSWFs modulation signals based on FFT/IFFT, which has lower complexity [13], i.e.,

$$S(\omega)=\sum_{i=0}^{gn-1}x(i+1)\psi_i(\omega) \tag{12}$$

where $\psi_i(\omega)$ represents the frequency domain waveform of the ith order PSWFs signal $\varphi_i(t)(i=0,1,\cdots,ng-1)$, and $x(i+1)\in\boldsymbol{X}$ represents the $(i+1)$th modulation symbol in $\boldsymbol{X}$. Then, the time-domain waveform of the modulated signal can be obtained using IFFT processing, i.e.,

$$s(t)=\sum_{i=0}^{gn-1}x(i+1)\varphi_i(t) \tag{13}$$

where $s(t)$ represents the time domain waveform of GMM-PSWFs-IM modulated signal.

3. Principle of GMM-PSWFs-IM signal detection based on ML

Fig. 4 shows the schematic diagram of GMM-PSWFs-IM modulation signal demodulation and detection at the receiver, including PSWFs signal detection (red dashed box), signal index detection, and modulation symbol inverse mapping (blue dashed box).

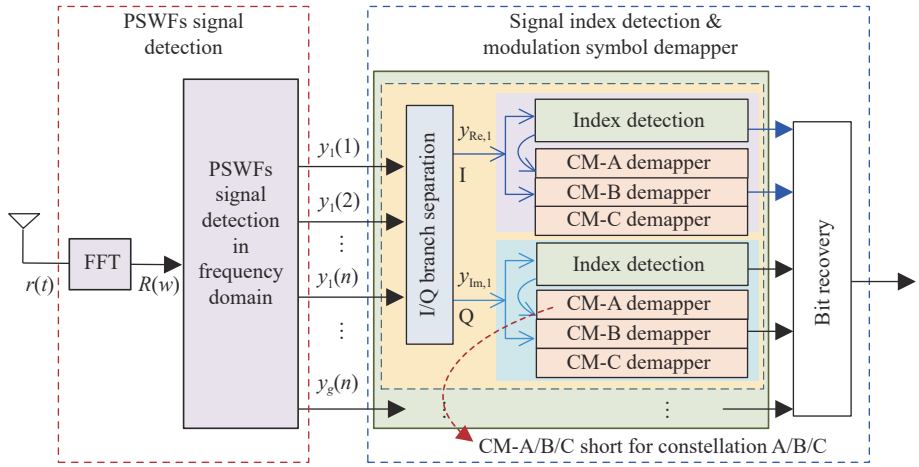

Fig. 4 Demodulation principle block diagram of GMM-PSWFs-IM

Therefore, the proposed method adopts the FFT-based PSWFs signal frequency domain detection method [13] for PSWFs signal detection. This involves acquiring the frequency domain waveform of the received signal using FFT. For the purpose of theoretical analysis and without loss of generality, assume that the channel is an additive white Gaussian noise (AWGN) channel. In this case, the Fourier transform of the received signal can be expressed as

$$R(\omega)=S(\omega)+N(\omega) \tag{14}$$

where $N(\omega)\sim \mathrm{N}(0,N_0/2)$ represents the frequency domain noise corresponding to AWGN, and N_0 represents the power spectral density of Gaussian white noise. According to the complete orthogonality of the PSWFs signal in the frequency domain, the cross-correlation function with the Fourier transform of the ith order PSWFs signal can be expressed as

$$r_i=<S(\omega)+N(\omega),\psi_i(\omega)>=x(i+1)+<N(\omega),\psi_i(\omega)>. \tag{15}$$

Then, a signal index detection method based on ML is adopted to detect the signal index, i.e.,

$$\left\{\hat{I}_{\mathrm{I},\alpha,k_i},\hat{s}_{\mathrm{I},\alpha,k_i},D_{\mathrm{I},\alpha,k_i}\right\}=\arg\min_{I_{\mathrm{I},\alpha,k_i},s_{\mathrm{I},\alpha,k_i}}\sum_{\gamma=1}^{n}\left|\mathrm{Im}\{[r]_{\upsilon,\upsilon}\}-s_{\mathrm{I},\alpha}(\upsilon)\right|^2, \tag{16}$$

$$\left\{\hat{I}_{\mathrm{Q},\alpha,k_i},\hat{s}_{\mathrm{Q},\alpha,k_i},D_{\mathrm{Q},\alpha,k_i}\right\}=\arg\min_{I_{\mathrm{Q},\alpha,k_i},s_{\mathrm{Q},\alpha,k_i}}\sum_{\gamma=1}^{n}\left|-\mathrm{Re}\{[r]_{\upsilon,\upsilon}\}-s_{\mathrm{Q},\alpha}(\upsilon)\right|^2, \tag{17}$$

where $D_{\mathrm{I/Q},\alpha,k_i}$ represents the Euclidean distance of

$\{\hat{I}_{\mathrm{I/Q},\alpha,k_i}, \hat{s}_{\mathrm{I/Q},\alpha,k_i}\}$, and $r \in \mathbf{C}^{ng\times 1}$ represents the modulation symbols corresponding to the received PSWFs signals of different orders. Then, based on the detected signal index, recover the bit information carried by the signal index. Finally, according to constellation A, constellation B, and constellation C, inverse mapping is performed on the modulation symbol to recover the bit information carried by the modulation symbol, and the two are combined to obtain all the bit information carried by the modulation signal.

4. System performance analysis

Given that the proposed GMM-PSWFs-IM can be degraded into other types of signal index modulation, such as signal index modulation with fixed activation signal number (i.e., the 2nd signal index silence, MCM-PSWFs-SGO[19]), generalized signal index modulation (i.e., the 1st signal index silence, constellation B silence, MCM-PSWFs GIM [22]), and traditional dual mode modulation (i.e., the 1st signal index silence, OFDM replacing PSWFs-MCM, GMM-OFDM-IM [24]), etc. Meanwhile, Wang et al. [19−21] discovered that the DM-MCM-PSWFs, MCM-PSWFs-SGO, and BIM-MCM-PSWFs outperform traditional orthogonal multi-carrier modulation based on PSWFs in terms of system SE and BER performance. Furthermore, Wang et al. [13,19] discovered that when comparing the performance of PSWFs-MCM based on PSWFs signals and OFDM based on sampling signals, modulation methods based on PSWFs-MCM outperform those based on OFDM. In addition, results [19,22] have obtained that power spectral density (PSD) and PAPR characteristics are the same when the number of signal paths and modulation symbol input number used for information transmission are the same. Also [20] agrees with the conclusion. Therefore, we do not do more analysis on the characters of PSD and PAPR.

This section compares the proposed method to the other three methods, DM-MCM-PSWFs, MCM-PSWFs-SGO, and BIM-MCM-PSWFs, in terms of system SE, BER performance, and signal index detection complexity.

4.1 Analysis of SE

Assuming that the time bandwidth product of PSWFs signals is $c=B/F$, when the symbol cycle is Q, the system SE of different modulation methods can be uniformly expressed as

$$\eta = Qm_e/[QT(B+F)] \tag{18}$$

where T represents the symbol period, m_e denotes the amount of information carried by a single symbol period modulation symbol. For different modulation methods, m_e is respectively

$$\begin{cases} m_{e,\mathrm{DM}} = 2g\left(\left\lfloor \log_2 C_n^k \right\rfloor + n\log_2 M\right) \\ m_{e,\mathrm{BIM}} = 2g\left(\left\lfloor \log_2 C_n^k C_k^m \right\rfloor + n\log_2 M\right) \\ m_{e,\mathrm{SGO}} = 2g\left(\left\lfloor \log_2 C_n^k \right\rfloor + k\log_2 M\right) \\ m_{e,\mathrm{GMM\text{-}IM}} = 2g\left(\left\lfloor \log_2 \left(C_n^k M^k\right)\right\rfloor + \lfloor (n-k)\log_2(1+M)\rfloor\right) \end{cases} \tag{19}$$

where DM represents DM-MCM-PSWFs, BIM represents BIM-MCM-PSWFs, SGO represents MCM-PSWFs-SGO, and GMM-IM represents GMM-PSWFs IM.

(i) In contrast to DM-MCM-PSWFs and MCM-PSWFs-SGO, the proposed method employs not only the dual signal index, but also the generalized signal index, which allows for an increase in the number of modulation symbol combinations. According to (8), when the above three methods have the same M, the proposed method has a higher SE. For example, when n=10, the proposed method improves system SE by approximately 32.0% at the expense of 1.69 dB BER performance sacrifice compared to DM-MCM-PSWFs, and improves system SE by approximately 69.3% at the expense of 2.87 dB BER performance sacrifice compared to MCM-PSWFs-SGO, as shown in Table 2, where bandwidth B is 1.44 MHz, frequency interval F is 15 kHz, value l is 4. Furthermore, when MCM-PSWFs-SGO uses higher-order constellation maps for modulation symbol mapping, the proposed method can improve SE and BER performance simultaneously with optimal parameter selection. For example, when M=4, the system SE and BER performance are improved by 41.2% and 0.77 dB, respectively.

Table 2 System SE of different MCM methods (BER=10^{-5})

Modulation method	g	n	k	m	SE/(bit/s/Hz)	(E_b/N_0)/dB	Improvement/%
BIM-MCM-PSWFs [21]	11	8	7	4	3.63	13.14	12.4
DM-MCM-PSWFs [20]	10	9	5	/	3.09	12.23	32.0
MCM-PSWFs-SGO-2PAM [19]	9	10	7	/	2.41	11.05	69.3
MCM-PSWFs-SGO-4PAM [19]	10	9	5	/	2.89	14.69	41.2
GMM-PSWFs-IM (the proposed method)	9	10	/	/	4.08	13.92	/

(ii) Compared with BIM-MCM-PSWFs, although both methods have undergone dual signal index, the proposed method adopts the idea of generalized signal index in the second signal index, which can further increase the number of modulation symbol combinations. Therefore, the system SE of the proposed method will be greater than that of BIM-MCM-PSWFs, when they are with the same M. For example, when n=10, the proposed method is able

to improve the system SE by about 12.4% at the expense of 0.78 dB BER performance, as shown in Table 2.

4.2 Analysis of BER performance

Because MED can visualize the system BER performance of modulation methods, it is chosen in this section to analyze the system BER performance of various modulation methods. It is worth noting that because the proposed method employs three constellation maps, the third of which is made up of peripheral constellation points, its MED is slightly larger than that of the other two constellation maps, and because only a small number of subcarriers in each group of subcarriers transmit the modulation symbols mapped by the third constellation diagram, its MED has a small and negligible impact on the system BER performance.

When the energy corresponding to each bit of information is E_b, the MED of different modulation methods can be represented as

$$\begin{cases} d^2_{\min,\ \mathrm{DM}}=\dfrac{24}{4(\log_2 2M_{\mathrm{DM}})^2-1}\cdot\dfrac{2\lfloor\log_2 C_n^k M_{\mathrm{DM}}^n\rfloor E_b}{n} \\ d^2_{\min,\ \mathrm{BIM}}=\dfrac{12}{4(\log_2 2M_{\mathrm{BIM}})^2-1}\cdot\dfrac{10n}{5n+20}\cdot \\ \qquad\dfrac{2\lfloor\log_2 C_n^1 C_{n-1}^m M_{\mathrm{BIM}}^n\rfloor E_b}{n} \\ d^2_{\min,\ \mathrm{SGO}}=\dfrac{12}{4(\log_2 M_{\mathrm{MCM}})^2-1}\cdot\dfrac{2\lfloor\log_2 C_n^k M_{\mathrm{SGO}}^k\rfloor E_b}{k} \\ d^2_{\min,\ \mathrm{GMM-IM}}=\dfrac{12}{4(\log_2 2M_{\mathrm{GMM-IM}})^2-1}\cdot\dfrac{10n}{5n+20}\cdot \\ \qquad\dfrac{2\lfloor\log_2 C_n^1 M_{\mathrm{GMM-IM}}^{2n-1}\rfloor E_b}{n} \end{cases} \tag{20}$$

where M represents the base number of modulation symbols for various index modulation methods.

(i) Compared with BIM-MCM-PSWFs, the ratio of EMD between the proposed method and BIM-MCM-PSWFs shows

$$\frac{d^2_{\min,\ \mathrm{GMM-IM}}}{d^2_{\min,\ \mathrm{BIM}}}=\frac{\lfloor\log_2 C_n^1 M_{\mathrm{GMM-IM}}^{2n-1}\rfloor}{\lfloor\log_2 C_n^1 C_{n-1}^m M_{\mathrm{BIM}}^n\rfloor}. \tag{21}$$

According to (10), the MED of the proposed method is very close to that of the BIM-MCM-PSWFs, but since the signal index scheme of the proposed method is generalized multiple index, the PSWFs signal number of the first and second constellation map cannot be roughly the same, and there is even a situation in which only the first or second constellation map is selected, resulting in an uneven distribution of the constellation points. This indicates that the proposed method improves system SE at the expense of sacrificing some BER performance. For example, when BER=10^{-5} and n=10, the proposed method achieves about 12.4% improvement in system SE at the expense of 0.78 dB BER performance compared to the BIM-MCM-PSWFs with parameters n = 8, k = 7, and M = 4, as shown in Fig. 5(b).

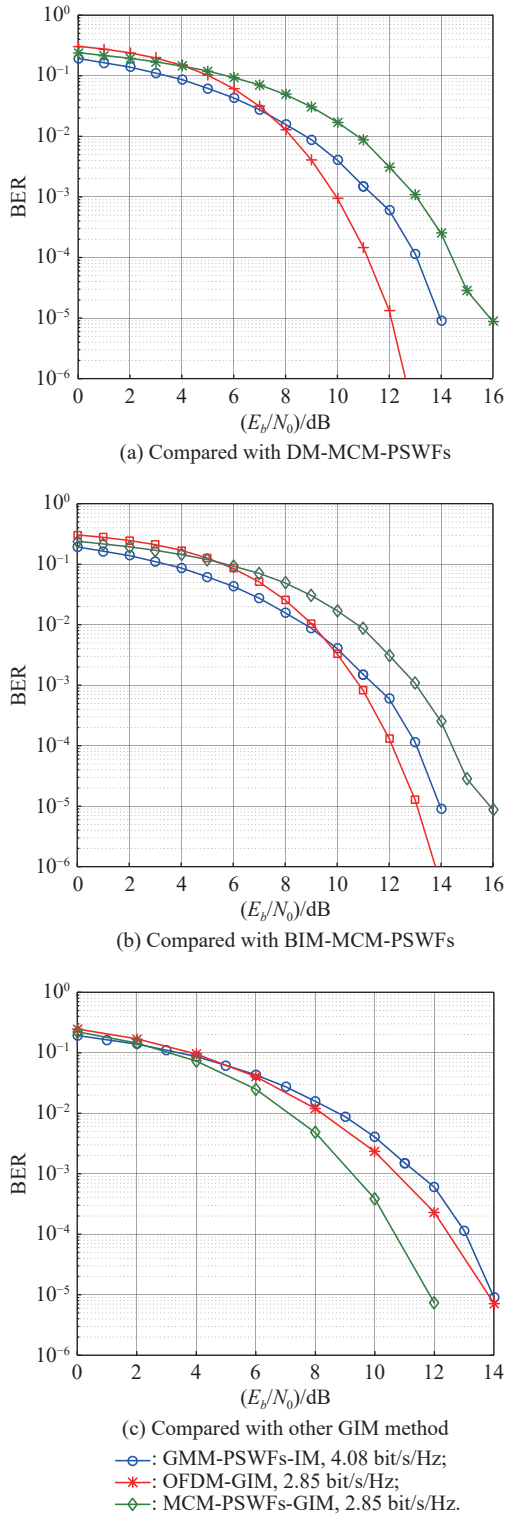

Fig. 5 System error performance of different modulation methods under AWGN channel

(ii) Compared with DM-MCM-PSWFs, the ratio of EMD between the proposed method and DM-MCM-PSWFs shows

$$\frac{d^2_{\text{min, GMM-IM}}}{d^2_{\text{min, DM}}}=\frac{4(\log_2 2M_{\text{DM}})^2-1}{4(\log_2 2M_{\text{GMM-IM}})^2-1}\cdot \frac{\lfloor \log_2 C_n^1 M_{\text{GMM-IM}}^{2n-1}\rfloor}{\lfloor \log_2 C_n^k M_{\text{DM}}^n\rfloor}\cdot\frac{5n}{5n+20}. \tag{22}$$

Meanwhile, [21] contends that the MED of BIM-MCM-PSWFs is smaller than that of DM-MCM-PSWFs, whereas the MED of the proposed method is smaller than that of BIM-MCM-PSWFs, indicating that the MED of the proposed method is smaller than that of DM-MCM-PSWFs. However, as the number of subcarriers n increases, the MEDs of BIM-MCM-PSWFs and DM-MCM-PSWFs are gradually approximated, and when the number of subcarriers n is large, the MEDs of the two are nearly identical. This means that under the assumption of a larger number of subcarriers n, the proposed method can improve system SE while sacrificing less BER performance. For example, when BER=10^{-5}, the proposed method (n=10) is able to achieve about 28.3% improvement in system SE at the expense of 1.72 dB BER performance compared to DM-MCM-PSWFs (n=8, k=4), as shown in Fig. 5(a).

(iii) Compared with MCM-PSWFs-SGO, the ratio of EMD between the proposed method and MCM-PSWFs-SGO shows

$$\frac{d^2_{\text{min, GMM-IM}}}{d^2_{\text{min, SGO}}}=\frac{4(\log_2 M_{\text{SGO}})^2-1}{4(\log_2 2M_{\text{GMM-IM}})^2-1}\cdot \frac{\lfloor \log_2 C_n^1 M_{\text{GMM-IM}}^{2n-1}\rfloor}{\lfloor \log_2 C_n^k M_{\text{SGO}}^k\rfloor}\cdot\frac{k}{n}\cdot\frac{10n}{5n+20}. \tag{23}$$

To more intuitively compare and analyze the difference between the system BER of MCM-PSWFs-SGO and the proposed method, 4-PAM is chosen as the constellation diagram for MCM-PSWFs-SGO and k=n−1 in BIM-MCM-PSWFs to ensure that the two systems have the same system SE. For larger n, k, the combination of (19) shows that the MED of the proposed method is greater than that of MCM-PSWFs-SGO, implying that it has a better BER performance. For example, when BER=10^{-5}, compared with MCM-PSWFs-SGO (n=8, k=6), the proposed method (n=10) can improve the system SE and BER performance by 12.4% and 1.80 dB, respectively, as shown in Fig. 5(b).

(iv) Compared to other methods of generalized signal index modulation. Fig. 5(c) compares the proposed method to MCM-PSWFs-GIM [22] and OFDM-GIM [25] in terms of system SE and BER performance. The simulation results show that the proposed method can sacrifice some BER performance in exchange for a significant increase in SE when compared to MCM-PSWFs-GIM and OFDM-GIM. For example, when BER=10^{-5} and n=10, the proposed method sacrifices 1.90 dB of system BER performance while improving SE by approximately 43.2% when compared to MCM-PSWFs-GIM, and sacrifices 0.20 dB of system BER performance while improving SE by approximately 43.2% when compared to OFDM-GIM.

(v) The comparison of system BER performance in Rayleigh channels. The system BER performance of the proposed method in Rayleigh channels is analyzed below to further demonstrate the practical application value of the proposed method in this paper. Given that the proposed method uses an I/Q branch, the following comparison analysis compares and analyses the differences in BER performance between the proposed method and the classical multiple-mode (MM)-OFDM-IM-IQ [26] and the optimized IQ-dimension-expanded multi-aligned multi-mode enhanced SIM OFDM (MP-OFDM-ESIM) [27], DM-MCM-PSWFs, and BIM-MCM-PSWFs, which also adopt I/Q branch.

i) Compared with DM-MCM-PSWFs and BIM-MCM-PSWFs, under Rayleigh channel, the BER performance of the proposed method is still consistent with the theoretical analysis results, which is sacrificing part of the BER performance in exchange for the improvement of SE. For example, when BER=10^{-3}, the SE is improved by 43.2% at the cost of sacrificing 3.55 dB of the system BER performance compared with DM-MCM-PSWFs, improved by 10% at the cost of sacrificing 0.72 dB of BER performance compared with BIM-MCM-PSWFs, as shown in Fig. 6(a).

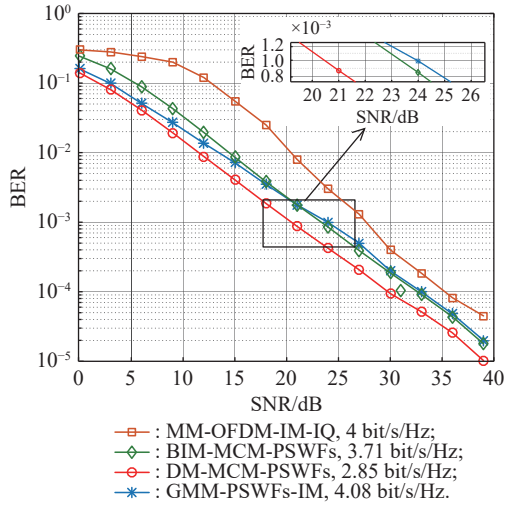

(a) Compared with MM-OFDM-IM, BIM-MCM-PSWFs and DM-MCM-PSWFs

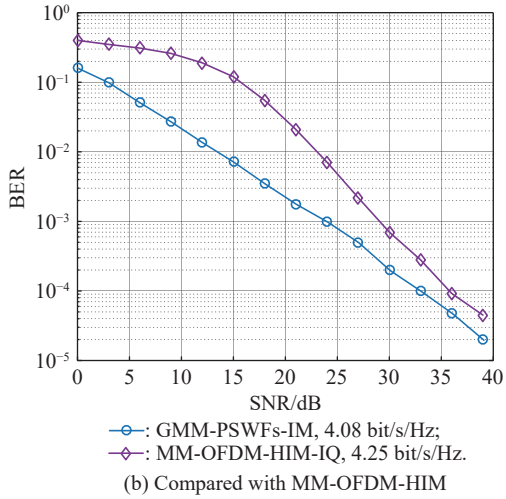

(b) Compared with MM-OFDM-HIM

Fig. 6 System error performance of different modulation methods under Rayleigh channel

ii) Compared to MM-OFDM-IM-IQ [28], the proposed method can achieve a significant improvement in the BER performance under Rayleigh channel when system SE is similar. For example, when BER=10^{-3}, the proposed method improves the system BER performance by 3.77 dB, as shown in Fig. 6(a).

iii) Compared with MM-OFDM-hybrid IM-IQ (MM-OFDM-HIM-IQ) [24], the proposed method is able to achieve a significant improvement in BER performance under Rayleigh channel when system SE is similar. For example, when BER=10^{-3}, the proposed method improves the system BER performance by 5.00 dB, as shown in Fig. 6(b).

4.3 Analysis of system complexity

Table 3 compares the proposed method's signal index detection multiplicative complexity to other modulation methods with a bandwidth of B=1.44 MHz and a frequency interval of F=15 kHz. The proposed method has a higher system complexity than that of other methods, such as DM-MCM-PSWFs and BIM-MCM-PSWFs, because it requires dual signal index and the second signal index uses generalized signal index. This implies that the proposed method's above performance advantages are obtained at the expense of an appropriate sacrifice of system complexity, but with continuous improvement of hardware level, the problem of high system complexity will be gradually solved.

Table 3 Signal index detection multiplication operation amount with 1.44 MHz bandwidth

Modulation method	Computational complexity	n	k	m	Operation amount
DM-MCM-PSWFs-ML [20]	$O(ng2^{\lfloor \log_2 C_n^k \rfloor})$	4	2	/	368
		9	4	/	5 760
BIM-MCM-PSWFs-ML [21]	$O(ng(2^{\lfloor \log_2 C_n^k \rfloor}+2^{\lfloor \log_2 C_k^m \rfloor}))$	4	3	2	552
		9	8	4	6 480
BIM-MCM-PSWFs-ML [21]	$O(ng(2^{\lfloor \log_2 C_n^k \rfloor}+2^{\lfloor \log_2 C_k^m \rfloor}))$	8	7	4	3 784
GMM-PSWFs-IM-ML (the proposed method)	$O(ng(2^{\lfloor \log_2 (C_n^k M^k) \rfloor+\lfloor (n-k)\log_2(1+M) \rfloor}))$	10	/	/	46 800

5. Conclusions

In this paper, a new index modulation method called GMM-PSWFs-IM is proposed. This method introduces generalized signal index on the basis of the original BIM-MCM-PSWFs. By employing a third constellation diagram for the dual signal indexing, the number of activated subcarriers for the 2nd signal index is no longer limited and the number of modulation symbol combinations increases.

In comparison to DM-MCM-PSWFs and BIM-MCM-PSWFs, the proposed method can improve system SE while increasing system computational complexity and BER performance. Under the same modulation base as MCM-PSWFs-SGO, it can achieve a dual improvement in SE and BER performance, resulting in better overall system performance. The proposed method outperforms the classical MM-OFDM-IM-IQ method in Rayleigh channels with similar system SE.

It is worth noting that the method still has room for improvement. Further efforts are suggested on how to select the optimal constellation diagram for a better system SE with less BER sacrifice. The optimization can also be proposed on how to obtain lower BER under low SNR. And how to optimize signal index detection to improve the overall BER performance will be a key question of future work.

References

[1] AMAKAWA S, ASLAM Z, BUCKWATER J, et al. White paper on RF enabling 6G-opportunities and challenges from technology to spectrum. https://biblio.ugent.be/publication/8704523.

[2] ZHANG Z Q, XIAO Y, MA Z, et al. 6G wireless networks: vision, requirements, architecture, and key technologies. IEEE Vehicular Technology Magazine, 2019, 14(3): 28–41.

[3] PREKSHA J, AKHIL G, NEERAJ K. A vision towards inte-

grated 6G communication networks: promising technologies, architecture, and use-cases. Physical Communication, 2022, 12(55): 101917.
[4] WANG C X, YOU X H, GAO X Q, et al. On the road to 6G: visions, requirements, key technologies, and testbeds. IEEE Communications Surveys & Tutorials, 2023, 25(2): 905–974.
[5] PANG J Y, WANG S, TANG Z, et al. A new 5G radio evolution towards 5G-advanced. Science China Information Sciences, 2022, 9(65): 191301.
[6] BASAR E, AYGOLU U, PANAYIRCI E, et al. Orthogonal frequency division multiplexing with index modulation. IEEE Trans. on Signal Processing, 2013, 61(22): 5536–5549.
[7] ASMORO K, SHIN S Y. RIS grouping based index modulation for 6G telecommunications. IEEE Wireless Communications Letters, 2022, 11(11): 2410–2414.
[8] LI S, XIAO L X, ZHANG X F, et al. Spatial multiplexing aided OTFS with index modulation. IEEE Trans. on Vehicular Technology, 2023, 72(6): 8192–8197.
[9] JAIN M, MAKKAR R, RAWAL D, et al. Dual-mode index modulation based OFDM system over NOMA networks. Physical Communication, 2021, 8(47): 101395.
[10] BUZZI S, ANDREA C D, LI D J, et al. MIMO-UFMC transceiver schemes for millimeter-wave wireless communications. IEEE Trans. on Communications, 2019, 67: 3323–3336.
[11] MICHAILOW N, MATTHE M, GASPAR I S, et al. Generalized frequency division multiplexing for 5th generation cellular network. IEEE Trans. on Communications, 2014, 62: 1205–1218.
[12] WANG Y, GUO Q, XIANG J H, et al. Doubly selective channel estimation and equalization based on ICI/ISI mitigation for OQAM-FBMC systems. Physical Communication, 2023, 8(59): 102120.
[13] WANG H X, LU F P, LIU C H, et al. Frequency domain multi-carrier modulation based on prolate spheroidal wave functions. IEEE Access, 2020, 8: 99665–99680.
[14] LU F P, WANG H X, LIU C H, et al. PSWFs frequency domain modulation and demodulation method. Journal of Electronics & Information Technology, 2020, 42: 1888–1895. (in Chinese)
[15] KEDAR K, NICHOLAS G. Sampling theory approach to prolate spheroidal wavefunctions. Journal of Physics, 2003, 36: 10011−10021.
[16] ZHEN J Q, WANG Z F. DOA estimation method for wideband signals by block sparse reconstruction. Journal of Systems Engineering and Electronics, 2016, 27(1): 20–27.
[17] TONG W, ZHU P Y. 6G: the next horizon: from connected people and things to connected intelligence. Cambridge: Cambridge University Press, 2021.
[18] MURUGESAN P P K, SIVABALIN V P G, NANJAN S M, et al. Orthogonal modes using prolate spheroidal wave function in holographic communication systems. Proc. of the International Conference on Signal Processing, Computation, Electronics, Power and Telecommunication, 2023. DOI: 10.1109/IConSCEPT57958.2023.10170733.
[19] WANG H X, LU F P, LIU C H, et al. Multi-carrier modulation scheme based on prolate spheroidal wave functions with signal grouping optimization. Scientia Sinica Informationis, 2020, 51(7): 1168–1182. (in Chinese)
[20] WANG H X, ZHANG L F, LU F P, et al. Multi-carrier index modulation based on prolate spheroidal wave functions with dual-mode. Journal of Electronics and Information Technology, 2022, 44(2): 694−701. (in Chinese)
[21] WANG H X, ZHANG L F, LU F P, et al. Multi-carrier index modulation based on prolate spheroidal wave functions with better multiple-mode. Journal of Electronics & Information Technology, 2022, 44(12): 4185–4193. (in Chinese)
[22] WANG H X, LU F P, LIU C H, et al. Multi-carrier modulation scheme based on prolate spheroidal wave functions with generalization index modulation. Scientia Sinica Informationis, 2021, 51(9): 1524–1539. (in Chinese)
[23] SLEPIAN D, POLLAK H O. Prolate spheroidal wave functions, fourier analysis, and uncertainty-I. The Bell System Technical Journal, 1961, 40(1): 43–46.
[24] WEN M W, LI Q, BASAR E, et al. Generalized multiple-mode OFDM with index modulation. IEEE Trans. on Wireless Communications, 2018, 17(10): 6531–6543.
[25] IRFAN M, AISSA S. Generalization of index-modulation: breaking the conventional limits on spectral and energy efficiencies. IEEE Trans. on Wireless Communications, 2021, 20(6): 3911–3924.
[26] WEN M W, BASAR E, LI Q, et al. Multiple-mode orthogonal frequency division multiplexing with index modulation. IEEE Trans. on Communications, 2017, 65(9): 3892–3906.
[27] ZHUANG L, DAI L, LIU S L, et al. Optimized scheme for spectrum and energy efficiency of multiple-mode OFDM with index modulation. Systems Engineering and Electronics, 2020, 42(3): 719–726. (in Chinese)
[28] ZHUANG L, DAI L, LIU S Z, et al. Optimized scheme for spectrum and energy efficiency of multiple-mode OFDM with index modulation. Systems Engineering and Electronics, 2020, 42(3): 719–726. (in Chinese)

Biographies

XU Zhichao was born in 1981. He received his M.S. degree from PLA University of Science and Technology in 2006. He is a lecturer in Naval Aviation University. His research interests are digital signal processing and waveform design for beyound 5G/6G.
E-mail: xzc8166@163.com

LU Faping was born in 1991. He received his Ph.D. degree from Naval Aviation University in 2021. He is a lecturer in Naval Aviation University. His research interests are digital signal processing, modern communication system and waveform design for beyound 5G/6G.
E-mail: lufaping@163.com

ZHANG Lifan was born in 1996. She received her M.S. degree from Naval Aviation University in 2021. She is an assistant engineer in Unit 92664 of the PLA. Her research interests are modern communication system and waveform design for beyound 5G/6G.
E-mail: 2758767464@qq.com

YANG Dongkai was born in 1972. He received his B.S. degree in electronic engineering from North University of China, Taiyuan, China, in 1994, and M.S. and Ph.D degrees in communication and information systems from Beihang University, Beijing, China, in 1997 and 2000, respectively. He is a professor in Beihang University. His research interests are global navigation satellite system and its applications.

E-mail: edkyang@buaa.edu.cn

LIU Chuanhui was born in 1987. He received his Ph.D. degree from Naval Aeronautical and Astronautical Engineering University. He is a lecturer in Naval Aviation University. His research interests are digital signal processing, statistical signal processing for wireless applications, waveform design for 5G and ultra wide band communication.

E-mail: lchgfy@163.com

KANG Jiafang was born in 1987. He received his Ph.D. degree from Naval Aeronautical and Astronautical Engineering University in 2014. He is an associate professor in Naval Aviation University in 2014. His research interests are modern multicarrier communications over fading channels, statistical signal processing for wireless applications, and signal design for the global navigation satellite system.

E-mail: 13791201919@163.com

AN Qi was born in 1994. She received her M.S. degree from Naval Aviation University in 2018. She is a teaching assistant in Naval Aviation University. Her research interests are modern communication system and waveform design for beyound 5G/6G.

E-mail: 18153567186@163.com

ZHANG Zhilin was born in 1997. He received his M.S. degree from Naval Aviation University in 2021. He is currently pursuing his Ph.D. degree with the Department of Aeronautical Communication, Naval Aviation University. His research interests are modern communication systems and network resource allocation.

E-mail: zzl19970811@163.com